Effects of laser-plasma interactions on terahertz radiation from solid targets irradiated by ultrashort intense laser pulses

Chun Li (李春),[1] Mu-Lin Zhou (周木林),[1] Wen-Jun Ding (丁文君),[1] Fei Du (杜飞),[1] Feng Liu (刘峰),[1] Yu-Tong Li (李玉同),[1,*] Wei-Min Wang (王伟民),[1] Zheng-Ming Sheng (盛政明),[1,2] Jing-Long Ma (马景龙),[1] Li-Ming Chen (陈黎明),[1] Xin Lu (鲁欣),[1] Quan-Li Dong (董全力),[1] Zhao-Hua Wang (王兆华),[1] Zheng Lou (娄铮),[3] Sheng-Cai Shi (史生才),[3] Zhi-Yi Wei (魏志义),[1] and Jie Zhang (张杰)[1,2,†]

[1]*Beijing National Laboratory of Condensed Matter Physics, Institute of Physics, CAS, Beijing 100190, China*

[2]*Key Laboratory for Laser Plasmas of the Ministry of Education of China and Department of Physics, Shanghai Jiao Tong University, Shanghai 200240, China*

[3]*Purple Mountain Observatory, Chinese Academy of Sciences, Nanjing 210008, China*

(Received 7 December 2010; revised manuscript received 16 May 2011; published 9 September 2011)

Interactions of 100-fs laser pulses with solid targets at intensities of 10^{18} W/cm^2 and resultant terahertz (THz) radiation are studied under different laser contrast ratio conditions. THz emission is measured in the specular reflection direction, which appears to decrease as the laser contrast ratio varies from 10^{-8} to 10^{-6}. Correspondingly, the frequency spectra of the reflected light are observed changing from second harmonic dominant, three-halves harmonic dominant, to vanishing of both harmonics. Two-dimensional particle-in-cell simulation also suggests that this observation is correlated with the plasma density scale length change. The results demonstrate that the THz emission is closely related to the laser-plasma interaction processes. The emission is strong when resonance absorption is a key feature of the interaction, and becomes much weaker when parametric instabilities dominate.

DOI: 10.1103/PhysRevE.84.036405 PACS number(s): 52.59.Ye, 52.25.Os

I. INTRODUCTION

Terahertz (THz) radiation has wide ranging applications in material screening, biological imaging, chemistry, medicine, etc. [1–4]. THz waves can be generated directly by illuminating different photoconductive antennas [5] and electro-optic crystals [6] with ultrashort laser pulses. These broadband pulsed THz sources have usually operated at high repetition frequency (above 1 kHz) with microwatt-to-milliwatt level average power.

High peak power terahertz sources are required for nonlinear studies [7], development of single-shot THz imaging systems [8], and THz pump-probe measurement of dynamics, etc. Conventional electron accelerators are used to generate intense THz radiation. Single-cycle coherent THz pulses with pulse energies as high as 100 μJ have been achieved recently from a linear accelerator [9]. Besides the large-scale facilities, there have been intense tabletop amplifier-laser-based THz systems employing large-area THz emitters. THz pulses with pulse energies of 0.8 μJ [10] and 1.5 μJ [11] have been obtained from large-aperture GaAs wafers and ZnTe crystals, respectively. By tilting the laser pulse intensity front, 30-μJ single-cycle THz pulses have been reached by phase-matched optical rectification using large-scale MgO:$LiNbO_3$ crystals [12]. On the other hand, laser-induced plasmas have attracted considerable interest in generating powerful THz pulses. Various alternative mechanisms for THz emission generation based on laser-plasma interactions have been proposed [13–15]. Relativistic electron beams from laser-plasma accelerators have been used to produce coherent THz radiation [16]. Alternatively, THz emission can be generated from femtosecond-induced breakdown of gases [17,18]. Through applying a certain "bias" provided by an external electric field [19,20] or an "optical second harmonic (SH) field" [21,22], such THz emission can be much increased.

THz pulses from femtosecond laser-induced plasmas in *solid* targets have also been demonstrated [17], [23]. Correspondingly two generations of mechanisms have been proposed. One involves the laser ponderomotive force, which accelerates electrons while ions are inertially confined due to their large mass in the short pulse duration [17]. Hence a large transient space-charge field is created, which will in succession give rise to THz radiation. However, this model is supposed to be more suitable to explain THz generation processes in underdense gas targets, which allow the laser pulses to propagate into the plasma and generate a longitudinal electron current. Another mechanism proposed is named "'antenna," in order to stress that the target size determines the emission spectrum of THz radiation [23]. In this model, only the electrons accelerated along the target surface by the laser field will produce THz radiation, i.e., the source of the THz radiation is a time-dependent current whose life time is equal to the ratio of half of the target size to the velocity of electrons. The spectrum of THz radiation from laser-driven plasmas generated on a copper wire was measured using free-space electro-optic sampling [24]. However, no clear evidence was found to show that the target size has any effect on the THz radiation spectrum.

The interaction of ultrashort laser pulses with plasmas which leads to the generation of THz radiation is a complex process. When femtosecond laser pulses propagate in plasmas, part of the laser energy is first transferred to the plasma through various absorption mechanisms [25]. Electron currents excited during the interaction will in succession give rise to THz radiation directly or indirectly. Hence it is expected that the THz emission is closely relevant with the laser absorption

*ytli@aphy.iphy.ac.cn,
†jzhang@aphy.iphy.ac.cn

mechanisms. Since the plasma has little time to expand during the main femtosecond laser pulse, the properties of the preformed plasma, especially its scale length, are of paramount importance for the description of ultrashort laser-plasma interactions. It has been observed that the principal absorption mechanisms transit from resonance absorption to parametric instabilities, such as two-plasmon decay (TPD) and stimulated Raman scattering (SRS), as the density scale length is increased [26]. Several experimental investigations have been reported to demonstrate that angular dependence of fast electrons and x-ray emission [27], as well as high harmonic generation [28] all depends strongly on absorption mechanisms, especially on the preplasma scale lengths. However, little experimental work has been dedicated to understand the effects of laser absorption on THz emission from laser-induced solid density plasmas. In this paper, we present experimental and numerical study of the preplasma effects on THz wave generation from solid targets by controlling the laser contrast ratio. We find that the THz radiation is strongly affected by the preplasma scale length.

II. EXPERIMENTAL SETUP

The experiments were performed using a Ti:sapphire laser system delivering 100-fs, 820-nm pulses at a repetition rate of 10 Hz. Before the main pulse there is a 4-ns amplified spontaneous emission (ASE) pedestal with an intensity contrast to the main pulse of 5×10^{-6}. By using saturable absorber filters, we can improve this contrast ratio to 3×10^{-8}. A small leakage light from the main pulse behind a reflective mirror was collected before the vacuum chamber for shot-to-shot laser parameter monitoring. The ASE was measured by an 8-Gb bandwidth oscilloscope and the spectrum by a fiber spectrometer (200–1100 nm). The linearly polarized laser pulse was focused onto the target using a $f/3.5$ off-axis parabolic mirror with an incidence angle of 67.5° to the target normal. The polarization of the incident light could be changed by a half-wave plate. We measured the focal spot at low energy with a microscope objective, and monitored it by an x-ray pinhole camera at high energy. The focal spot contained 35% of the energy within 5 μm full width at half maximum (FWHM), resulting in a maximum intensity of 5×10^{18} W/cm^2. The targets were single-side polished copper plates with a thickness of 1 mm. For each laser shot a fresh surface was provided by shifting the targets.

The experimental setup is illustrated in Fig. 1(a). We collected the THz emission in the specular reflection direction into a solid angle of 0.07 sr by a pair of polymethylpentene (TPX) lenses with apertures of 50 mm and focal lengths of 150 mm. TPX is optically transparent in UV, visible, and far-infrared ranges, and has an index of refraction of ~1.46, which is weakly dependent on wavelength. The emission was first collimated and then refocused onto a pyroelectric detector, which has a relatively flat voltage response between 0.3 to 21 THz with an average responsivity of $\sim 10^4$ V/W. A signal caught by the pyroelectric detector is shown in Fig. 1(b), which has a typical pulse duration of ~1 ms at FWHM. A single-side polished high resistivity silicon (HR-Si) wafer with a diameter of 100 mm was applied as a beam splitter in the path of the collimated THz beam. It allowed a transmittance of ~50% of the THz beam and meantime reflected the visible light for spectrum measurement. The reflected light was directed out of the chamber through a pair of selective absorption glasses, QB5 and QB11, and then collected by another visible spectrometer (200–1100 nm) with a solid angle of 10^{-3} sr. Figure 1(c) shows a typical reflected light spectrum, where the second and three-halves harmonics of the fundamental light ω_0 are shown clearly. A γ-ray measurement system, which consists of a NaI detector, a photomultiplier, and an amplifier, was used to measure radiation above 150 keV. In order to eliminate the noise caused by the random γ-ray scattering and enhance the ratio of signal to noise, the detector was fully enclosed by a Pb cylinder with a 10-mm-diam hole.

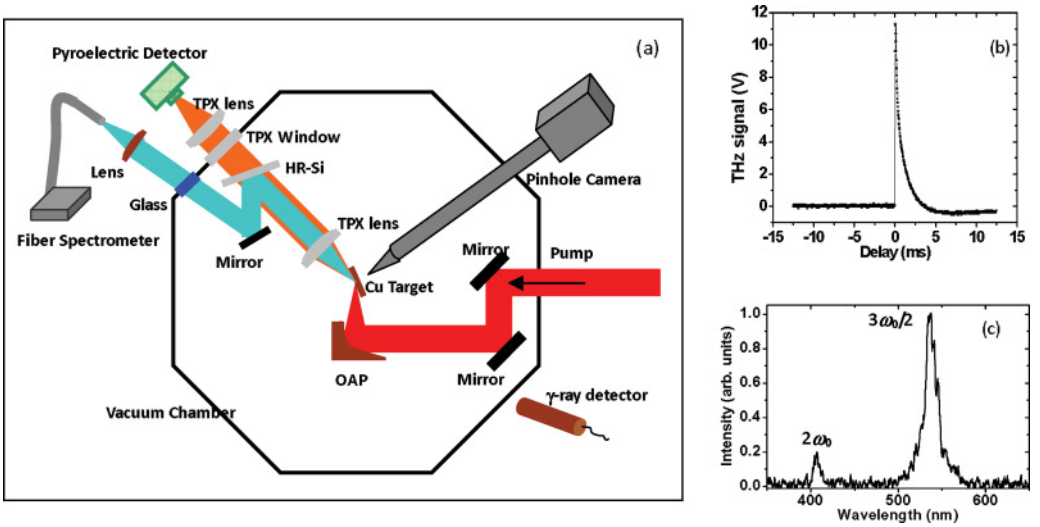

FIG. 1. (Color online) (a) Schematics of the experimental setup. THz emission in the specular reflection direction was measured by a pyroelectric detector, and the spectrum of the reflected light investigated by a fiber spectrometer. A typical signal recorded by the pyroelectric detector as well as the reflected light spectrum is shown in (b) and (c), respectively.

III. MEASUREMENT, DATA ANALYSIS, AND DISCUSSIONS

In our experiments, for p-polarized irradiation at the angle of incidence of 67.5°, the observed energy of THz emission with respect to the laser contrast ratio is shown in Figs. 2(a) and 2(b) for $a_0 = 0.7$ and 1.0. Here a_0 is the normalized laser field amplitude given as $a_0 = 8.53 \times 10^{-10}(I\lambda_0^2)^{1/2}$, where I is the laser intensity in W/cm^2 and λ_0 is the laser wavelength in μm. The two values are chosen to represent subrelativistic and relativistic laser intensities. Plasmas produced at these intensities are expected to show significant influence of the steepness of the laser pulse, which is normally determined by the temporal shape and the intensity contrast ratio of the laser pulses. If the ASE background-to-peak contrast ratio is large enough, plasmas will be formed by the laser pulse front before the main pulse arriving (usually the threshold value of optical breakdown intensity of matter is on the order of $10^{10} - 10^{11}$ W/cm^2). In our experiments, the contrast ratio of the ASE to main peak is changed from 2×10^{-8} to 5×10^{-6}, resulting in preplasmas with different scale lengths. With both laser intensities, as depicted in Figs. 2(a) and 2(b), THz emission falls when the laser contrast ratio becomes poorer (i.e., the intensity ratio between ASE and peak becomes larger). The observed THz yield drops by a factor of 10 when the laser contrast ratio is changed from the order of 10^{-7} to 10^{-6}, whereas it declines slowly when the laser contrast ratio is changed from 10^{-8} to 10^{-7}. Along with the THz emission we measured the γ-ray signal. The γ ray also decreases when the ASE pedestal goes larger.

To understand the underlying absorption mechanisms, we measured the reflected light spectrum with THz emission. Spectra were collected for ~100 shots under each laser contrast ratio, and the intensity of every characteristic peak was averaged. The averaged intensities of the second harmonic signal on laser contrast ratio for $a_0 = 0.7$ and 1.0 are shown in Figs. 2(c) and 2(d). The corresponding values for the three-halves harmonic are given in Figs. 2(e) and 2(f). The SH signals show the same trend of decreasing as THz and γ-ray emission when the laser contrast ratio becomes poorer. However, the three-halves harmonic signals are much different; they first increase, reach a maximum, and decrease again.

The reflected light spectra are depicted in Fig. 3 for $a_0 = 0.7$ [Fig. 3(a)] and 1.0 [Fig. 3(b)]; frames from top to bottom represent the three laser contrast ratio conditions corresponding to Figs. 2(a) and 2(b). We can see clearly from the spectra that when the laser contrast is on the order of 10^{-8}, the SH signals are presented for both intensities, which is evidence of strong resonance absorption. When the laser contrast is changed to 10^{-7}, the $2\omega_0$ components are depressed, while emission near $3\omega_0/2$ dominates. This indicates that TPD is occurring close to $n_c/4$, where n_c is the critical density given as $n_c = 1.1 \times 10^{21}(\mu\text{m}/\lambda_0)^2\text{cm}^{-3}$. At larger scale lengths of preplasmas, emission at $3\omega_0/2$ becomes weak again. The reason may be that the SRS below the quarter critical density exceeds the TPD and becomes the dominant process of laser-driven instabilities [25]. Since the Raman scattering is always expected to generate downshifted light, the frequency of which exceeds the spectral range of the spectrometer, we have not seen clear signatures of SRS in the spectra.

Our measurements of the frequency spectra of the reflected light along with THz emission indicate that the THz emission is closely related to the laser-plasma interaction process. With our experimental conditions for p-polarized irradiation at oblique incidence, THz emission is strongest when the intense SH generation indicates that resonance absorption is dominant. At the laser contrast ratio ~10^{-7}, when TPD takes place, both of the THz and SH emissions are decreased. If the laser contrast ratio decreases further, the second harmonic disappears and the THz emission drops sharply.

To confirm the experimental observations on the transition of absorption mechanisms for different preplasma scale lengths for p-polarized light, we have carried out a series of numerical particle-in-cell (PIC) simulations in two-dimensional (2D) geometry. In the simulations, we use targets composed of a high-density region with a density of $6n_c$, and a preformed plasma with exponential decreasing density distributions with

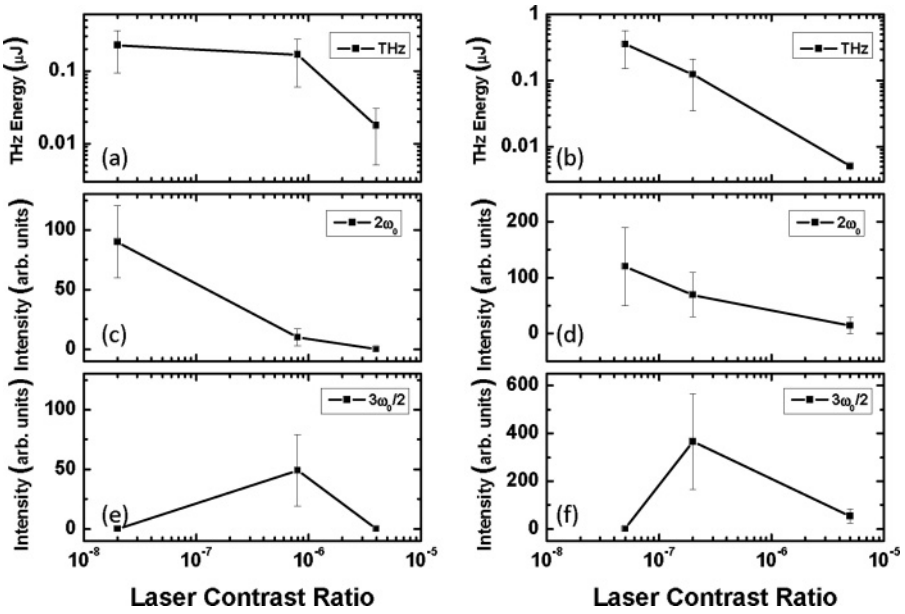

FIG. 2. Dependence of terahertz emission from Cu targets on laser contrast ratio for $a_0 =$ 0.7 (a) and 1.0 (b) by p-polarized laser pulses at an incidence angle of 67.5°. The corresponding averaged $2\omega_0$ intensities on laser contrast ratio are shown in (c) and (d) for $a_0 = 0.7$ and 1.0, and $3\omega_0/2$ in (e) and (f), respectively. Each point represents an average of ~100 laser shots.

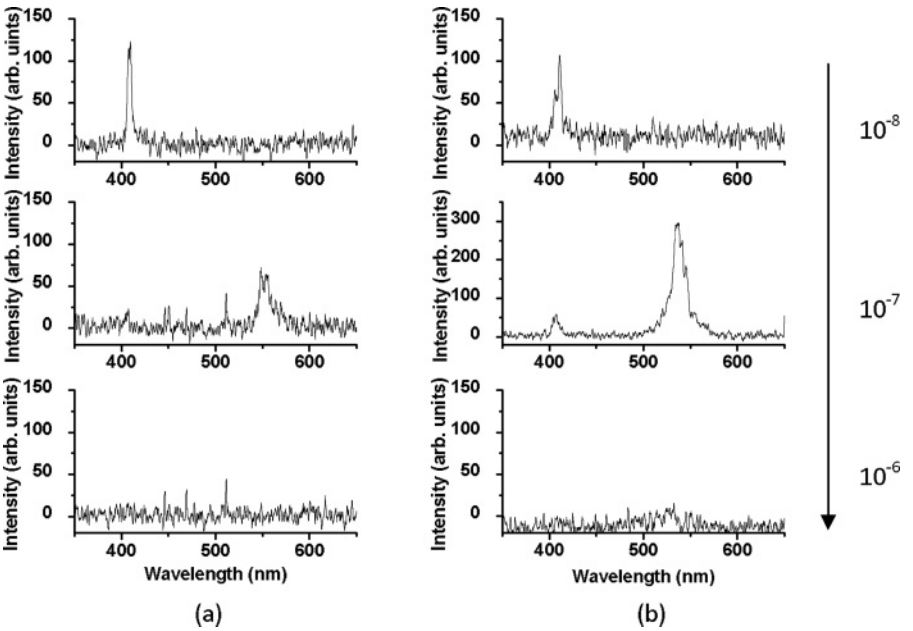

FIG. 3. Frequency spectra of reflected light for *p*-polarized incidence of laser pulses at an angle of incidence of 67.5° for $a_0 = 0.7$ (a) and 1.0 (b). Frames from top to bottom represent different laser contrast conditions, in the order of 10^{-8}, 10^{-7}, and 10^{-6}, respectively. Corresponding THz yields are given in Figs. 2(a) and 2(b).

variable scale length L. The temporal profile of the *p*-polarized laser pulse is a sine-squared shape with a duration of 30 laser cycles and the spatial profile is a Gaussian cross section with a beam diameter of $10\lambda_0$. The simulations are carried out for both $a_0 = 0.7$ and 1.0. The results do not show much difference for these two intensities. The spectra of the reflected light for $a_0 = 0.7$, integrated over transverse space, are shown in Fig. 4. The same variation in second and three-halves harmonics in reflected light spectra are seen as that observed in experiments. The high harmonic emission decreases as the scale length increases, as depicted from Figs. 4(a)–4(d). In the case of no preplasma and small preplasmas for Figs. 4(a) and 4(b), only the fundamental and second harmonic of ω_0 are clear. For $L \geqslant \lambda_0$, the $3\omega_0/2$ component rising from the TPD occurs. At larger scale lengths, such as $L = 4\lambda_0$, both resonance absorption and TPD disappear. No emission of high harmonics of ω_0 or $\omega_0/2$ is observed, while the low frequency components, which are signatures of SRS, dominate. From these simulation results, we can conclude that the case with high THz emission yields in our experiments corresponds to the plasma scale lengths less than a laser wavelength.

For comparison, *s*-polarized light with the laser contrast ratio $\sim 10^{-8}$ was also used to generate THz radiation in our experiments. The yield of THz radiation drops by a factor of 4 compared with that by *p*-polarized light at the same optical pulse energy. In contrast to the reflected spectra depicted on the top line of Figs. 3(a) and 3(b), where the second harmonic generation is clear, no obvious SH emission is observed for

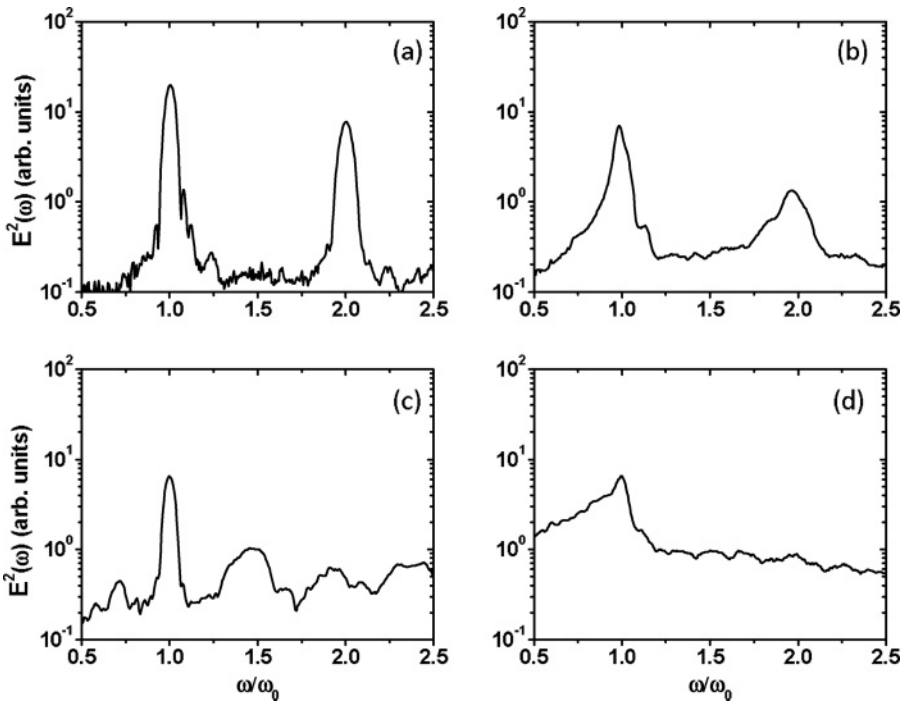

FIG. 4. Frequency spectra of reflected light from 2D PIC simulations for *p*-polarized incidence of laser pulses at an incidence angle of 45° for $a_0 = 0.7$. From (a) to (d), the corresponding plasma density scale lengths are $L = 0, 0.5\lambda_0, \lambda_0$, and $4\lambda_0$, respectively.

s-polarized light. The strong enhancement in the production of THz and SH emission in the case of *p*-polarized laser light indicates a more efficient laser-plasma coupling. As suggested in Ref. [29], electron plasma waves generated by the resonance process account for almost all of the total SH yield for *p*-polarized laser light in the case of small preplasmas. For *s*-polarized light, there is no component of the electric vector along the direction of the plasma density gradient. The local electric field is no longer resonantly enhanced and, in agreement with experimental observations, no SH signal is detected. This is further evidence that the resonance absorption, which dominates the laser-plasma interaction process in the laser contrast ratio of 10^{-8} for *p*-polarized incidence, is favorable for THz radiation generation.

It is interesting to compare our experimental results with previous experiments on the role of preplasmas for THz generation. It has been shown that there is a drop of one order in THz yield reported by Hamster *et al.* [30] when the laser contrast ratio is improved from 5×10^{-4} to 2.5×10^{-6}. However, our experiments reported here show that the energy of THz emission grows with the laser contrast ratio in the range of 10^{-6}–10^{-8}. These experimental results suggest that the dependency of THz emission on plasma scale lengths imparted by the ASE may be not a monotonous function. There might be more than one generation mechanism contributing to the total THz yield in the process of femtosecond laser-plasma interaction in solid targets. According to our experimental and analysis results, high THz yield is suggested corresponding to a relatively small preplasma density scale length. The hot electron generation, in this case due to resonance absorption, should play an important role for the observed THz emission. The transient electron currents rising from the hot electron generation and return currents from the background electrons established at the target surface could lead to such emission [31,32]. This is different from the experiments by Hamster *et al.*, where much longer plasma scale lengths exist and emission from plasma oscillations driven by the laser pondermotive force dominates. We can see that the preplasma parameters are of paramount importance for the THz emission output and should be carefully designed. A carefully controlled prepulse with a varied temporal separation between the main pulse, as well as a time-resolved measurement of the THz radiation, will help us to learn more about the generation mechanisms and optimize the THz wave from solid density plasmas.

IV. SUMMARY

We have measured the THz emission in the specular reflection direction with linearly polarized laser pulses irradiated on solid targets. THz emission is found to be strongly dependent on the laser-plasma interaction processes, especially on the density scale lengths of preplasmas. With relatively small preplasma density scale lengths, such as less than a laser wavelength, when resonance absorption dominates, THz emission generation is effective. At larger preplasmas when parametric instabilities such as TPD and SRS occur, the THz emission decreases significantly. The plasma condition should be carefully chosen to optimize and control the generation of the THz wave in front of targets.

ACKNOWLEDGMENTS

We thank C. L. Zhang for calibrating the detectors and filters, and L. Wang for fruitful discussions. This work is supported by the National Nature Science Foundation of China (Grants No. 10925421 and No. 10734130), and National Basic Research Program of China (973 Program) (Grants No. 2007CB815101 and No. 2007CB310406).

[1] B. Ferguson and X.-C. Zhang, Nat. Mater. **1**, 26 (2002).
[2] C. A. Schmuttenmaer, Chem. Rev. **104**, 1759 (2004).
[3] P. H. Siegel, IEEE Trans. Microwave Theory Tech. **52**, 2438 (2004).
[4] M. Tonouchi, Nat. Photonics **1**, 97 (2007).
[5] D. H. Auston, K. P. Cheung, and P. R. Smith, Appl. Phys. Lett. **45**, 284 (1984).
[6] L. Xu, X.-C. Zhang, and D. Auston, Appl. Phys. Lett. **61**, 1784 (1992).
[7] P. Gaal, K. Reimann, M. Woerner, T. Elsaesser, R. Hey, and K. H. Ploog, Phys. Rev. Lett. **96**, 187402 (2006).
[8] Z. Jiang and X.-C. Zhang, Opt. Lett. **23**, 1114 (1998).
[9] Y. Shen, T. Watanabe, D. A. Arena, C. C. Kao, J. B. Murphy, T. Y. Tsang, X. J. Wang, and G. L. Carr, Phys. Rev. Lett. **99**, 043901 (2007).
[10] D. You, R. R. Jones, P. H. Bucksbaum, and D. R. Dykaar, Opt. Lett. **18**, 290 (1993).
[11] F. Blanchard, L. Razzari, H.-C. Bandulet, G. Sharma, R. Morandotti, J.-C. Kieffer, T. Ozaki, M. Ried, H. F. Tiedje, H. K. Haugen, and F. A. Hegmann, Opt. Express **15**, 13212 (2007).
[12] A. G. Stepanov, L. Bonacina, S. V. Chekalin, and J.-P. Wolf, Opt. Lett. **33**, 2497 (2008).
[13] Z.-M. Sheng, K. Mima, J. Zhang, and H. Sanuki, Phys. Rev. Lett. **94**, 095003 (2005).
[14] H.-C. Wu, Z.-M. Sheng, and J. Zhang, Phys. Rev. E. **77**, 046405 (2008).
[15] W.-M. Wang, Z.-M. Sheng, H.-C. Wu, M. Chen, C. Li, J. Zhang, and K. Mima, Opt. Express **16**, 16999 (2008).
[16] W. P. Leemans, C. G. R. Geddes, J. Faure, Cs. Tóth, J. van Tilborg, C. B. Schroeder, E. Esarey, G. Fubiani, D. Auerbach, B. Marcelis, M. A. Carnahan, R. A. Kaindl, J. Byrd, and M. C. Martin, Phys. Rev. Lett. **91**, 074802 (2003).
[17] H. Hamster, A. Sullivan, S. Gordon, W. White, and R. W. Falcone, Phys. Rev. Lett. **71**, 2725 (1993).
[18] S. Tzortzakis, G. Méchain, G. Patalano, Y.-B. André, B. Prade, M. Franco, A. Mysyrowicz, J.-M. Munier, M. Gheudin, G. Beaudin, and P. Encrenaz, Opt. Lett. **27**, 1944 (2002).
[19] T. Löffler, F. Jacob, and H. G. Roskos, Appl. Phys. Lett. **77**, 453 (2000).
[20] A. Houard, Y. Liu, B. Prade, V. T. Tikhonchuk, and A. Mysyrowicz, Phys. Rev. Lett. **100**, 255006 (2008).

[21] T. Bartel, P. Gaal, K. Reimann, M. Woerner, and T. Elsaesser, Opt. Lett. **30**, 2805 (2005).

[22] K. Y. Kim, A. J. Taylor, J. H. Glownia, and G. Rodriguez, Nat. Photonics **2**, 605 (2008).

[23] A. Sagiska, H. Daido, S. Nashima, S. Orimo, K. Ogura, M. Mori, A. Yogo, J. Ma, I. Daito, A. S. Pirozhkov, S. V. Bulanov, T. Zh. Esirhepov, K. Shimizu, M. Hosoda, Appl. Phys. B **90**, 373 (2008).

[24] Y. Gao, T. Drake, Z. Chen, and M. F. Decamp, Opt. Lett. **33**, 2776 (2008).

[25] W. L. Kruer, *The Physics of Laser-Plasma Interactions* (Addison-Wesley, New York, 1988).

[26] J. Zhang, Y. T. Li, Z. M. Sheng, Z. Y. Wei, Q. L. Dong, and X. Lu, Appl. Phys. B Lasers Opt. **80**, 957 (2005).

[27] S. Bastiani, A. Rousse, J. P. Geindre, P. Audebert, C. Quoix, G. Hamoniaux, A. Antonetti, and J.-C. Gauthier, Phys. Rev. E **56**, 7179 (1997).

[28] M. Zepf, G. D. Tsakiris, G. Pretzler, I. Watts, D. M. Chambers, P. A. Norreys, U. Andiel, A. E. Danger, K. Eidmann, C. Gahn, A. Machacek, J. S. Wark, K. Witte, Phys. Rev. E **58**, R5253 (1998).

[29] L. A. Gizzi, D. Giulietti, and A. Giulietti, Phys. Rev. Lett. **76**, 2278 (1996).

[30] H. Hamster, A. Sullivan, S. Gordon, and R. W. Falcone, Phys. Rev. E **49**, 671 (1994).

[31] Y. T. Li, X. H. Yuan, M. H. Xu, Z. Y. Zheng, Z. M. Sheng, M. Chen, Y. Y. Ma, W. X. Liang, Q. Z. Yu, Y. Zhang, F. Liu, Z. H. Wang, Z. Y. Wei, W. Zhao, Z. Jin, and J. Zhang, Phys. Rev. Lett. **96**, 165003 (2006).

[32] Y. T. Li, C. Li, M. L. Zhou, W. M. Wang, F. Du, W. J. Ding, X. X. Lin, F. Liu, Z. M. Sheng, L. M. Chen, J. L. Ma, X. Lu, Q. L. Dong, Z. H. Wang, Z. Y. Wei, and J. Zhang, e-print arXiv:1106.0543v1 [physics.optics].